Published in final edited form as:
J Control Release. 2013 December 28; 172(3): . doi:10.1016/j.jconrel.2013.10.016.

In Vivo Biodistribution of siRNA and Cisplatin Administered using CD44-Targeted Hyaluronic Acid Nanoparticles

Shanthi Ganesh[1,2], **Arun K. Iyer**[1], **Florence Gattacceca**[1,3], **David V. Morrissey**[2], and **Mansoor M. Amiji**[1,*]

[1]Department of Pharmaceutical Sciences, School of Pharmacy, Bouvé College of Health Sciences, Northeastern University, Boston, MA 02115, USA

[2]Novartis Institutes for Biomedical Research Inc., Cambridge, MA 02139, USA

[3]Department of Pharmacokinetics, EA4215, Faculté de Pharmacie, Université, Montpellier 1, 34093 Montpellier Cedex 5, France

Abstract

Multidrug resistance (MDR) is a significant problem in the clinical management of several cancers. Overcoming MDR generally involves multi-modal therapeutic approaches that integrates enhancement of delivery efficiency using targeted nano-platforms as well as strategies that can sensitize cancer cells to drug treatments. We recently demonstrated that tandem delivery of siRNAs that downregulate anti-apoptotic genes overexpressed in cisplatin resistant tumors followed by therapeutic challenge using cisplatin loaded in CD44 targeted hyaluronic acid (HA) nanoparticles (NPs) induced synergistic antitumor response in CD44 expressing tumors that are resistant to cisplatin. In the current study, a near infrared (NIR) dye-loaded HA NPs was employed to image the whole body localization of NPs after intravenous (i.v.) injection into live mice bearing human lung tumors that were sensitive and resistant to cisplatin. In addition, we quantified the siRNA duplexes and cisplatin dose distribution in various tissues and organs using an ultra-sensitive quantitative PCR method and inductively coupled plasma-mass spectrometry (ICP-MS), respectively, after i.v. injection of the payload loaded HA NPs in tumor bearing mice. Our findings demonstrate that the distribution pattern of the siRNA and cisplatin using specifically engineered CD44 targeting HA NPs correlated well with the tumor targeting capability as well as the activity and efficacy obtained with combination treatments.

Keywords

Hyaluronic acid; siRNA; cisplatin; nanoparticles; tumor targeting; combination therapy; multidrug resistance

*Corresponding author: Tel. 617-373-3137, Fax 617-373-8886, m.amiji@neu.edu.

6. Conflict of Interest

The authors declare that they have no conflict of interest.

1. Introduction

Multidrug resistance (MDR) is a significant problem in the clinical management of several cancers [1]. Overcoming MDR generally involves multi-modal therapeutic approaches that integrates enhancement of delivery efficiency using targeted nano-platforms as well as strategies that can sensitize cancer cells to drug treatments [2–4]. It has been demonstrated in our previous study that tandem siRNA treatment followed by cisplatin regimen reversed resistance and significantly increased the tumor cell death [5]. The efficacy study was based on delivering siRNA and cisplatin using specifically engineered CD44 targeting hyaluronic acid (HA) nanoparticles (NPs) that home to CD44 receptor overexpressing cisplatin resistant tumors [5, 6]. In order to understand the correlation between the activity and the distribution levels in the tumors and various non-target organs and tissues, in the current study, the siRNA and cisplatin loaded HA NPs were tracked and quantified by using various ultra-sensitive methods. Furthermore a near IR (NIR) dye indocyanine green (ICG) was loaded in the HA NPs to image the whole body distribution of the NPs in live tumor bearing mice. ICG is a water soluble, amphiphilic near infrared (NIR) dye that strongly absorbs and fluoresces in the NIR region exhibiting a favorable absorption and emission maxima (λ_{max}) at 780 and 820 nm respectively [7–9]. Since most of the biomolecules and tissue do not absorb and emit in the NIR region, the fluorescence of ICG is relatively free of any background interferences or tissue auto-fluorescence and gives a more reliable signal for optical imaging applications. In addition, ICG has been approved for clinical use by the United States Food and Drug Administration [10]. In several studies, ICG has been used as a fluorescence contrast agent in diagnostic imaging for early detection of superficial tumors and many other medical applications [11]. ICG has also been explored extensively for numerous applications including NIR imaging in preclinical studies such as tracking its distribution in different tissues [12]. One of the issues with the use of free ICG is its short half-life and rapid clearance from circulatory system [7]. In the current study, we have encapsulated ICG in the HA NPs that were previously used to deliver siRNA to tumors as part of an independent efficacy and safety study [5, 6].

In addition to monitoring the NPs loaded with NIR dye, the distribution pattern of active therapeutic payload, such as siRNA, is also important in understanding the efficacy that was observed during the combination treatment. For this purpose the siRNA was encapsulated in identical HA NPs that were used in the efficacy studies and an ultra-sensitive PCR method was utilized to quantitate siRNA at ~picogram levels present in different tissues, including tumor tissue, several hours after the treatment [13, 14].

Since cisplatin loaded HA NPs was also used in our combination treatments, it is important to understand its distribution when encapsulated in HA NPs [15]. After i.v injection of the free cisplatin solution or cisplatin loaded HA NPs in tumor bearing mice, the cisplatin content was quantified in various tissues and plasma using a highly sensitive and reliable inductively coupled plasma-mass spectrometry (ICP-MS) method that permits accurate determination at or below the parts per million levels in native samples [16]. Indeed, direct coupling of the HPLC column to an ICP-MS is known to detect specific mass of interest for platinum at nanogram levels. This way it leads to specific and sensitive detection with little background interference from complex biological matrices. It has been reported previously that the use of this sensitive and versatile method allows unequivocal identification and quantitation of platinum complexes including cisplatin [16]. HPLC-ICP-MS technique has gained popularity recently for detecting trace elements in biological and clinical samples.

2. Materials and Methods

2.1. Chemicals and Reagents

Highly purified and well characterized grade of sodium hyaluronate with an average molecular weight of 20 kDa was obtained from Lifecore Biomedical Co. (Chaska, MN). Poly(ethylene imine) (PEI, MW~10,000 Da) was obtained from Polysciences Inc. (Warrington, PA). Sulfo-NHS was purchased from Thermo Scientific Corp (Billerica, MA), monofunctional polyethyleneglycol amine (PEG_{2k}-NH_2, MW=2000 Da) was purchased from Creative PEG Works (Winston Salem, NC). Indocyanine green (ICG), *cis*-diamineplatinum(II) dichloride (≥99.9%, cisplatin) and 1,8-diaminooctane (ODA) were purchased from Sigma-Aldrich Chemical Co (Milwaukee, WI). Other reagents for synthesis were obtained at high purity (>99%) from Sigma-Aldrich Chemical Co (Milwaukee, WI) or Acros Organics (Thermo Fisher, Pittsburgh, PA) and used without further purification. O-phenylenediamine was purchased from Wako Chemicals (Tokyo, Japan). AgPath-ID One step RT-PCR kit part# AM1005 was purchased from Invitrogen (Carlsbad, CA) to perform RT-PCR.

2.2. Cell Lines and Tumor Models

Human non-small cell lung cancer (NSCLC) A549 and small cell lung cancer (SCLC) H69 cell lines were obtained from ATCC (Manassas, VA). The corresponding resistant cell lines ($A549^{DDP}$ and H69AR) were obtained from Massachusetts General Hospital (Boston, MA) and ATCC (Manassas, VA), respectively. Cells were grown in RPMI medium supplemented with 10 % FBS. Animal procedures were performed according to a protocol approved by Northeastern University, Institutional Animal Care and Use Committee (NU-IACUC). Tumor models were developed in nude mice obtained from Harlan Laboratories (South Easton, MA). For the tumor model development, 5–6 week old nude mice were injected subcutaneously (s.c.) with A549 (5×10^6 cells + Matrigel®), $A549^{DDP}$ (1×10^7 cells), H69 (1×10^7 cells), H69Ar (1×10^7cells + Matrigel®) tumor cells, under the right shoulder. Tumor volume was measured twice a week to monitor the tumor growth.

2.3. ICG-Loaded HA Nanoparticles for Optical Imaging

In order to understand the biodistribution of HA NPs, ICG, an amphiphilic carbocyanine dye that strongly absorbs and fluoresces in the NIR region was encapsulated in the NPs. The NPs were prepared according to a method employed to construct siRNA loaded HA NPs reported before [6]. HA-PEI and HA-PEG derivatives used in this study were also synthesized as described previously [6]. Briefly, an equal volume of HA-PEI (900 μl, 3mg/ml in PBS) and HA-PEG (900ul, 3 mg/ml in PBS) were mixed, vortexed and kept at room temperature for 5 min. Then 200 μl of ICG solution (0.5mg/ml in water) was added to the above mixture, vortexed and kept at room temperature for 15–20 min. The solutions were then dialyzed against phosphate buffered saline (PBS) overnight using 10 kDa MW cut-off membrane (Spectrapore, Spectrum Labs, San Diego, CA). In order to determine the encapsulated ICG content in the NPs, a standard curve was initially run with the dye alone at different concentrations. The absorbance was measured at 780 nm for the standard curve and for determining the ICG content in the NPs. Tumor bearing mice were developed as described before and the study commenced when the tumors reached an average size of ~200 mm^3. The NPs were then injected i.v. into mice bearing A549, $A549^{DDP}$, H69 and H69AR tumors using the tail vein. Mice were imaged at 10 min, 4 h, 10 h, and 24 h after the injection to monitor the distribution of the NPs using IVIS Xenogen Imaging System (Xenogen Corporation, Alameda, CA) (Ex: 785 nm, Em: 820 nm). Along with these formulations, the free ICG in PBS (at identical encapsulated concentration) was also injected into mice bearing A549 tumors to compare the distribution of the free dye.

2.4. siRNA Quantitation in Tissues

Survivin silencing siRNA duplex was encapsulated in HA-PEI/HA-PEG NPs as described before [6]. Briefly 90 μl (3 mg/ml in PBS) of HA-PEI was mixed with 90 μl (3 mg/ml in PBS) of HA-PEG and incubated for 15 min at room temperature. Then 20 μl of 0.5 mg/ml survivin siRNA (in PBS) was added to the above mixture and vortexed well and incubated for additional 15 min at room temperature. The particle size and zeta potentials were measured using a Zetasizer (Zetasizer Nano-S, Malvern Instruments, UK). These NPs were injected into mice (n=3/ group) bearing cisplatin resistant lung tumors ($A549^{DDP}$) at 0.5 mg/kg for 3 days. After 1 h, 6 h, and 24 h following the last injection, blood samples and several major organs namely, liver, spleen, lung, heart, kidney and tumors were collected. The organs were then homogenized using Qiogen tissue Lyser (Qiagen, Germantown, MD) to prepare tissue lysates. The homogenized tissue lysates were subsequently diluted at 1:1000 to prepare dilute samples. Using the appropriate reverse primer, anti-primer and the tissue lysate, the annealing step was run initially followed by RT-PCR. The survivin siRNA sequence, reverse primer, forward primer, and an anti-primer sequence are listed below.

Survivin siRNA:

Sense: 5′GGmCGmUAAGAmUGAmUGGAmUmUmUmUmU3′

Antisense: 5′AAAUCmCAUmCAUCUmUACGCCmUmU3′

Primers

Reverse: GGAAGCCGAC**AAGGCGTAA**

Forward: /56-FAM/ACTCCCTCCCTCGATTT **AAATCCATCATCT**

Anti-primer: AAATCGAGGGAGGGAG/3BHQ_1/

As a first step, the siRNA was denatured and annealed to the RT primer (6 μl diluted siRNA and 18 μl reverse primer, 100 nM). siRNA was denatured by incubating at 95 °C for 5 min. Primers were then annealed by 2 min incubation at 80, 70, 60 and 45 °C with 4 °C hold. Then the reverse trancription reaction was carried out as follows. A master mix was made by mixing the following components: RT-PCR buffer (6.25 μl), forward primer, (10 μM, 0.12 μl), reverse primer (10 μM, 0.12 μl), antiprimer (100 μM, 0.12 μl), 25X RT-PCR enzyme (0.5 μl) and water (1.5 μl).

A total of 8.5 μl of this master mix was then mixed with 3.5ul of sample and ran the PCR at the following listed conditions: 50 °C (10 min), 9 °C (10 min), 40 cycles, 95°C (15 sec), 45 °C (60 sec). The amplified siRNAs were finally detected and quantitated by running a standard curve using lysate from untreated mouse tissue and spiked with known siRNA concentrations.

2.4. Cisplatin Quantitation in Tissues

For the quantitation study, cisplatin was first encapsulated in HA NPs. The HA-ODA and HA-PEG derivatives and the method to encapsulate cisplatin in HA-ODA with and without PEG was performed as described before [6]. Briefly, to fabricate the cisplatin/HA-ODA NPs, 90 μl (10 mg/ml in water) HA-ODA derivative was mixed with 10 μl (10 mg/ml) cisplatin solution (in DMSO). The complex was incubated at room temperature for 15 min and dialyzed against PBS using dialysis membrane (10 kDa MW cut-off, Spectrapore, Spectrum Labs, San Diego, CA) to get rid of the un-encapsulated cisplatin. In addition to these NPs, another set of NPs were also fabricated by including HA-PEG. For this purpose, 90 μl of HA-ODA (10 mg/ml in water) was initially mixed with 90 μl of HA-PEG (10 mg/ml in water) and incubated for few minutes at room temperature. Then 20 μl of cisplatin (10 mg/ml in DMSO) was added to the above mixture and vortexed well, incubated for 15 min

at room temperature followed by dialysis as described above. A well-established colorimetric method was used to determine encapsulated cisplatin concentration using O-phenylenediamine [17].

Tumors were grown as described and when they reached the size of ~100–150 mm^3, they were randomized into 4 groups (n=3/group) for the study. Cisplatin-encapsulated in HA-ODA and HA-ODA/HA-PEG NPs were then i.v. injected (tail vein) in mice bearing cisplatin resistant $A549^{DDP}$ tumors at 1 mg/kg dose. Free cisplatin solution was also injected in its conventional form at the same dose along with the NPs to get a comparative tissue distribution. After 6 h and 24 h following a single i.v. dose, blood and tissues were collected for platinum (Pt) analysis by ICP-MS. Blood samples were collected in heparinized tubes and centrifuged to get the plasma. Tissue samples such as liver, spleen, lung, kidney, heart, brain and tumor were harvested at the same time points. All the samples were processed to measure the sum total (encapsulated + released or protein bound and unbound) Pt for the NP formulations of cisplatin and for total (protein bound and unbound) Pt for free cisplatin. Samples were digested initially to get the free Pt in the lysate. Plasma samples were digested by adding 100 μl 70 % HNO_3 and 100 ng/ml Iridium solution to 50 μl plasma and heated for 1.5 h at 100 °C. Subsequently the mixture was then diluted to 1 ml with deionized water (Barnstead Nanopure, Thermo-Barnstead, Hampton, NH). For tissue processing, about 40–80 mg tissues was sectioned and recorded for exact weight. Digestion of those tissues samples were carried out as described for plasma samples and the final volume of those lysates was adjusted to get 2 ml with deionized water. The samples were subsequently used for ICP-MS analysis. In parallel, the standard curves for Pt and iridium solutions were also run. Iridium is used as the instrument internal standard and the concentrations are calculated based on the response ratio of platinum counts/second (cps) vs. iridium standards. The calculated platinum concentration is then regressed further using the ratio of Pt concentration observed and iridium internal standard ratio fit on a linear regression equation of 1/x.

2.5. Data Analysis

Statistical analysis was performed using GraphPad Prism software® (GraphPad Software Inc., CA) to determine if there is any significant difference between organ concentrations also between delivery systems. The two tailed unpaired t-test was used to compare the mean values ± standard errors; p values < 0.05 were considered statistically significant.

3. Results and Discussion

3.1. Biodistribution Analyses of ICG-Encapsulated HA Nanoparticles by *In Vivo* Imaging

We previously demonstrated that lung cancer cells such as A549 and its resistant counterpart $A549^{DDP}$ expressed saturating levels of CD44 and thus exhibited efficient gene downregulation when treated with siRNA encapsulated CD44 targeting HA NPs [6]. However, the apparent lower level expression of CD44 on H69AR (~ 90 %) and H69 (~60 %) cells led to lower level activity/knockdown in H69AR and almost no activity in H69 cells even at higher siRNA concentrations. Based on these findings, we focused our earlier efforts on downregulating the overexpressed genes present in the resistant $A549^{DDP}$ tumors using the appropriate therapeutic siRNAs and reversed the resistance in those tumors [5]. In the current study, our goal was to look at the distribution pattern of the HA NP loaded with cisplatin or siRNA and correlate its distribution pattern with the efficacy results observed previously. We were also interested in exploring the HA NP localization to tumors that are known to overexpress CD44 (A549/$A549^{DDP}$) and compare the results with tumors that express lower levels of CD44 receptors (H69/ H69AR).

To this end, we first evaluated the whole body NP distribution in live animals using NIR dye, ICG encapsulated in the HA NPs. For preparation of the ICG loaded HA-PEI/HA-PEG NPs, a similar method used to encapsulate siRNA was employed as described in the experimental section. These NPs have similar characteristics as presented by the siRNA encapsulated NPs (Table 1A). The particle size of HA-NP loaded with ICG was in the range of ~ 200 nm and displayed a negative surface charge/zeta potential of ~ −15 mV. However, the encapsulation of ICG in these particles was only 25% and the initial dose was calculated accordingly, to match with siRNA dosing.

The ICG loaded NPs were then i.v. injected in A549, $A549^{DDP}$, H69 and H69AR tumor bearing mice at a dose that is equivalent to the dose that was used in the efficacy study. The NPs were found to be stable during circulation on intravenous (i.v.) injection and its NIR signal was measured at different time points to capture the distribution pattern (Table 1B) in live mice. As expected, a strong NIR signal was initially observed throughout the whole body of mice in all 4 types of tumors at 10 min due to circulation of ICG loaded NPs in the blood after tail vein injection. At 4 h time point, majority of the signal was detected in the liver and spleen region of all the mice (the major organs of macromolecular accumulation, disintegration and clearance by the hepatobiliary system). In addition, the A549 tumor location also had a signal as seen in Fig. 1A. None of the other tumors had traceable amount of fluorescence at this time point. At 10 h, the signal in A549 tumors still persisted. However, the overall signal intensity was diminished throughout the body except in tumors for all the mice, possibly due to disintegration of the HA NPs and ICG release followed by rapid elimination. Interestingly, there was a clear fluorescence NIR signal detected in $A549^{DDP}$ tumors at 10 h (Figure 1A). However, no signal was detected in H69 or H69AR tumors at any time points tested (Figure 1B). At 24 h, there was no detectable fluorescence signal in any organ or tissue of all the mice (data not shown). These results corroborate the low CD44 receptor expression levels and the poor activity of HA NPs in H69 and H69 pair as seen earlier [6].

The distribution of ICG dye alone was also monitored over that period of time to compare its localization with that of the NP encapsulated counterpart. When free ICG was injected in A549 tumor bearing mice, the overall intensity of the signal was much lower than the signal that was observed in mice that received HA-NP/ICG as early as 10 min post injection. This was more evident at the 4 h time point (the only area detected was the liver/spleen, but not in tumors, Figure 1C). At 10 h, the majority of the signal in the liver disappeared possibly due to recirculation and clearance. Similar clearance patterns have been reported by other groups as well [18, 19]. Bahmani *et al.*, recently reported that after i.v. injection of free ICG in healthy mice, the signal was detectable in the liver as early as 3 minutes post-injection, reaching a peak level between 5 and 10 min, indicative of a rapid hepatic clearance from the systemic circulation, while the fluorescence signal in the liver was found to increase up to 60 min time point after NP administration [18]. Zheng et al., underlined that the relatively short circulation time of the free ICG *in vivo* could be attributed to fluorescence quenching of free ICG in physiological environments [19]. Consistent with our observations, Zheng *et al.*, also reported that free ICG could not be detected in the tumor at any time point from 0.5 to 24 h, although free ICG was still detectable in the intestinal region at 8 h post-injection. These results supported the previously described clearance pathway involving exclusive uptake by hepatic parenchymal cells and subsequent biliary excretion [20]. The higher and longer existing signal observed in mice that had HA NP/ICG treatment suggests that the HA NPs were stable in circulation and the ICG remained intact inside the NPs, protected from hepatic parenchymal cellular uptake. This distribution study with ICG clearly demonstrated that the NPs targeted tumors expressing saturating levels of CD44. However there was no signal detected in tumors that express lower than saturating levels of CD44 suggesting that a threshold level of CD44 expression is necessary for the NPs to bind and internalize via the

receptor mediated endocytosis. The late signal appearance in the resistant $A549^{DDP}$ tumors is consistent with our previous siRNA dependent knockdown data, which showed an increased survivin and bcl-2 knockdown after 72 h than at 24 h time point[5].

3.2. An Anti-Primer Quenching Based PCR Method to Quantify siRNA in Tissues

For the siRNA distribution and quantification study, the survivin siRNA that was used previously in the combination efficacy studies was encapsulated in identical HA-PEI/HA-PEG NPs (size: ~90–100 nm and charge: −15 mV). Since we demonstrated previously that we were able to efficiently deliver survivin siRNA to resistant $A549^{DDP}$ tumors and reverse the resistance, we were interested in looking at the distribution of the same siRNA in mice bearing identical tumors. After three i.v. injection of 0.5 mg/kg siRNA doses (in HA NP) into tumor bearing mice, blood and tissues samples were collected for siRNA quantitation at 1 h, 6 h and 24 h post last administered dose (Figure 2A). For the accurate siRNA quantitation, the anti-primer quenching based real time PCR method was utilized, as described in the experimental section [13]. In this method, a fluorescently labeled PCR primer was designed to anneal to the template RNA and to a universal anti-primer. Following the initial PCR, the temperature is lowered to allow the anti-primer to bind to the unincorporated primer to quench its fluorescence. Since this will not bind to the double stranded PCR product, there will be an increased fluorescent signal detected.

The siRNA was quantitated in each tissue and the % input dose per whole organ was calculated based on the starting siRNA dose as shown in Figure 2B. Liver showed about ~33.4 and 32.2 % of the injected dose at 1 h and 6 h. It was slightly reduced ($p<0.05$) at 24 h time point (~13.4 %). Similar pattern was detected in spleen as well, from ~22.8 % ID at 1 h to ~17.4 % at 24 h ($p=0.08$). The higher signal in liver and spleen corroborated the observation from the ICG study. About 2–3 % of input siRNA dose was detected in kidneys. The siRNA was also detected in tumor lysates but at a lower level compared to liver, spleen and kidney (0.5–1% ID), though still at a significantly higher level than in lung, heart and brain ($p<0.02$). Interestingly, the levels found in tumor at 24 h was significantly higher than the levels found at earlier time points ($p<0.05$) and this is consistent with higher ICG signal observed at later time point in resistant lung ($A549^{DDP}$) tumors. Levels found in lung and heart was very low (0.2–0.5 %), but still in the detectable range. The levels detected in plasma were even lower (~ 0.01– 0.004 % ID), suggesting that siRNA does not remain in plasma, but contrarily distributes quickly and widely into other organs that correlate well with the high levels measured in liver and spleen (which together contain more than 50 % ID at 1 h). Jiang *et al.*, similarly reported higher siRNA levels in liver and kidney, when compared to tumor, while lower levels were measured in lung and heart, 24 h post i.v. administration of Cy3-siRNA/PEI-HA complexes [21]. Surprisingly, these nano-complexes accounted for very low levels of siRNA in the spleen, lower than in any other organs studied, contrary to our HA formulations that exhibited very high spleen levels. However, the high spleen level in our case is consistent with high levels of CD44 expression in the spleen, as reported in many other studies [22, 23].

To estimate the rate of siRNA washout, we calculated the ratio of C_{last}/ C_{max}, i.e., siRNA concentration at the last time point (24 h) divided by the maximum concentration achieved at any time point (Figure 2C). In a given organ, the lower the ratio the higher the washout of siRNA from that organ (or the shorter the residence time of siRNA in that organ). In liver, where concentrations reached higher levels, the ratio was the lowest (0.402), suggesting that the siRNA would not remain long in the liver. This value was close to the plasma value (0.457), suggesting that concentrations in plasma and liver might evolve in parallel. The ratio was higher in spleen, lung and kidney (0.665, 0.622 and 0.724 respectively), indicating that siRNA would remain longer in those organs than in liver and plasma. The decrease in

siRNA concentrations has however started in those organs at 24 h. Contrarily, tumor and heart displayed a ratio of 1, which means that the C_{max} reported here was at 24 h, and consequently that the decrease in siRNA concentrations may not have started yet at 24 h time point, leading to an accumulation of siRNA in those organs. This result in tumor is consistent with higher ICG signal observed at later time point in resistant lung ($A549^{DDP}$) tumors, and could explain the results obtained in the efficacy study in these tumor models, in which the gene knockdown was much higher at 72 h or 120 h compared to an earlier (24 h) time point. The prolonged accumulation in heart is contrarily not a favorable event regarding possible toxicity. Future studies of this treatment strategy should probably include a later time point (72 h), so as to determine if the accumulation in heart will continue, followed by an evaluation of cardiac toxicity. However, this concern should be moderated to low due to the low level of siRNA found in the heart (Cmax around 0.3%).

3.3 Cisplatin Distribution Correlates with siRNA and Nanoparticle Distribution

Since we previously demonstrated a combination effect of siRNA and cisplatin mediated reversal of drug resistance, we were interested in looking at the distribution pattern of cisplatin during treatment as well. In order to achieve this objective, cisplatin was encapsulated in a functionally variant HA derivative (HA-ODA) primarily due to the hydrophobic nature of the cisplatin, and the difficulty it poses in encapsulation to form water soluble nanoparticles. As such, encapsulation of small molecule drug such as cisplatin in hydrophilic HA polymer or PEI derivatized HA is highly challenging. Thus we introduced fatty acid side-chains onto HA backbone to encapsulate cisplatin by self-assembly as discussed earlier [6]. This formulation previously delivered cisplatin to resistant lung tumors and demonstrated efficacy [5]. Additionally, we fabricated NPs containing both PEG modified HA (HA-PEG) and HA-ODA lipid modified version to assess if the PEG component could improve longer residence and achieve better tumor delivery. The physical characteristics of these two types of HA NPs were very similar (size: ~400–425 nm and charge: ~−25 mV (Table 2A). Since the maximum cisplatin encapsulation that could be achieved was ~18–20 % (w/w) in both the NPs, the doses were calculated accordingly. In the study, these two NPs containing cisplatin were tested along with free cisplatin solution for comparisons. All three formulations were injected i.v. as a single dose of 1 mg/kg cisplatin concentration. The tissues and plasma were collected at 6 h and 24 h post injection for cisplatin quantitation as shown in Table 2B. The samples were processed and analyzed by ICP-MS to quantitate the % input/injected dose per gram of tissue as shown (Figure 3). The ratio of 24 h concentration to 6 h concentration (C24h/C6h) was calculated and considered as a measure of the residence time of cisplatin in the tissue (Table 3). It was found that for all formulations, the most exposed organs were found to be the liver, kidney and spleen, while cisplatin levels were very low in the heart and the brain. Tumor, lung and plasma accumulation were intermediate. Although the delivery systems used for cisplatin and siRNA were not exactly the same, the distribution pattern observed for cisplatin was very similar to the results observed for the siRNA distribution study, probably because the major contributing factor is attributed to the bulk property of HA as well as NP surface characteristics, which also dictates tumor targeting (based on CD44 receptor overexpression).

As expected, the cisplatin plasma concentration at 6 h was enhanced by HA NP formulations, when compared to free cisplatin solution (3.3 and 3.0% ID/mL for HA-ODA and HA-ODA-PEG respectively, versus 1.8% for cisplatin solution, $p<0.05$). However, the C24h/C6h ratio was very low for HA-ODA NP (0.323) when compared to HA-ODA/HA-PEG NP (0.736) and free cisplatin solution (0.568), indicating that the concentration decreased rapidly for HA-ODA NP. Consequently, at 24 h, the levels in HA-ODA/cisplatin NP treated mice went down to the same level as that of free drug (cisplatin) solution treated

mice, while the mice that had HA-ODA/HA-PEG NP treatment displayed around twice as much (~ 2.2%) cisplatin levels than the free cisplatin solution and HA-ODA/cisplatin NP treatment (~1%) ($p<0.05$). The higher plasma residence time for PEGylated NPs has been extensively described in the literature, and attributed to the stealth characteristics of PEG coated NPs and their diminished uptake by the reticulo-endothelial system (RES) [24–26].

On the other hand, although the cisplatin concentration in the tumors of HA-ODA NP treated mice was lower than the levels exhibited by HA-ODA/HA-PEG NP treated mice (~1% ID/g versus ~1.5% ID/g respectively) at 6 h, they were not significantly different ($p=0.2$). Similarly, the cisplatin levels were slightly higher for HA-ODA NP treated mice at 24 h (~1.2% ID/g) compared to the HA-ODA/HA-PEG NP treated mice (~0.9%), but not statistically different However, the kinetics of the cisplatin accumulation seemed to be different for both NPs. Over the period of time, cisplatin continues to accumulate in the tumor of HA-ODA NP treated mice, with a C24h/C6h ratio of 1.21, but the cisplatin levels seem to decrease when HA-ODA/HA-PEG NP formulation was used for cisplatin delivery (ratio of 0.630), leading to a lower concentration at 24 h (~0.9 % ID/g). Again this difference is not statistically significant. However, if the trend continues, then the levels might reach a point at which there will be significant differences. Also, the trend will be more prominent if the study is run with larger number of mice and it may be suggesting that the HA-ODA NPs may be accumulating slowly into the tumors over a period of time, whereas the ODA/PEG NPs although accumulated rapidly, may start to clear out sooner. For the free cisplatin solution administration, the 6 h tumor concentration was the lowest (0.6 % ID/g), but tumor concentration increased between 6 h and 24 h (C24/C6 ratio of 1.6), allowing tumor concentration at 24 h to reach similar levels to that obtained for HA-ODA/HA-PEG NP administrated group (~0.9 % ID/g). However, with regard to overall distribution profile, free cisplatin solution lead to a low tumor accumulation, hence underlining the interest of the targeted NP approach for tumor selective delivery[27].

With regard to safety, the free cisplatin solution led to a rather lower level accumulation in the main off-target organs when compared with HA NPs. A striking exception is the spleen, in which, the concentration of cisplatin at 24 h was approximately 4-fold higher compared to the levels found in the spleens of NP treated mice (~4.5% ID/g versus ~1% ID/g, $p<0.01$)), making spleen the highest exposed organ at 24 h, at a cisplatin level similar to the levels in the kidneys. This higher accumulation of cisplatin in the spleen was demonstrated by a C24/C6 ratio of 3.650. An increase of the spleen cisplatin levels leading to high spleen exposure was also observed and reported by Comenge *et al.* [28]. However, we did not observe any adverse toxicity in mice or drastic variation in the animal body weights during the *in vivo* efficacy study. This observation may partly be due to the very low cisplatin dose used by us (1 mg/kg). The most striking results of our previous studies were the tumor suppression using the siRNA/cisplatin combination treatments even at these low doses of cisplatin as opposed to 10 mg/kg cisplatin doses generally used [29].

The HA NPs overall led to higher organ exposure and it is correlated to higher plasma concentrations. However, the biodistribution pattern was different for both NP types. After HA-ODA/HA-PEG NP administration, the cisplatin levels, while decreasing in the spleen and the kidneys between 6 h and 24 h (C24/C6 ratio of 0.321 and 0.832 respectively), it increased tremendously in liver (C24/C6 ratio of 1.65, $p<0.05$)), leading to the highest concentration measured in this study (9% ID/g), and raising concern about liver accumulation and toxicity of this formulation. After HA-ODA administration, liver concentration however decreased between 6 h and 24 h, with a ratio C24/C6 of 0.88, although still remaining at high levels (5%ID/g), but significantly lower than the levels detected in HA-ODA/HA-PEG NP treated mice ($p<0.05$). However as discussed above, we did not observe any adverse toxicity in any mouse groups (liver enzymes and histology) in

the efficacy studies. The cisplatin levels also decreased in the spleen (ratio of 0.496) of HA-ODA treated mice and were similar to those obtained after HA-ODA/HA-PEG NP treatment. In the kidney of HA-ODA treated mice, concentrations increased between 6 h and 24 h (ratio of 1.46), raising some concern about kidney accumulation and toxicity with this treatment, as with the free cisplatin solution. However, levels were lower at 6 h (4% ID/g, $p<0.05$) or at similar levels at 24 h (5.8% ID/g, $p=0.4$) compared to the levels found in HA-ODA/HA-PEG NP treated mice (7.65%ID/g and 6.3%ID/g). Taken together, these cisplatin tumor distribution data are consistent with the siRNA and ICG distribution studies, and allow us to explain the combination efficacy we saw previously.

In addition, He et al [30] have recently demonstratedhow the size and surface charge of the NPs play a major role on cellular uptake and biodistribution. Their well-defined particles with 150 nm size and −15 mV charge accumulated most efficiently in the tumors. It was also shown in the study that larger size particles of 500 nm and a charge of −25 mV, didn't accumulate as efficiently as the smaller ones in the tumors, instead they accumulated in organs like liver, spleen and in some cases in lung too, most likely due to the uptake by the macrophages present in those organs (via phagocytosis). This information corroborates the observation with our NPs as well.. HA-PEI/ HA-PEG NPs that are in the smaller size range (~90–100 nm, ~−15 mV) and (~200 nm, −15 mV) most likely accumulated in the tumors (~0.5–1% of the input siRNA dose was detected in the tumors).

The HA-ODA and HA-ODA/HA-PEG systems that we used for cisplatin delivery on the other hand, falls in the larger particle size category (~400 nm, −25mV). This NP size and charge data correlates with the larger particles with higher charge data in He et al's study. These NPs are likely to be accumulating at lower levels in tumors than the smaller particles described for siRNA/ICG delivery (we detected only ~0.2–0.3 % of the input dose in the tumors). Another observation from our study was that the HA-ODA/HA-PEG/cisplatin NPs, unlike the the HA-ODA/ cisplatin NPs, seemed to be accumulating more in the liver suggesting that the PEGylated particles might have been taken by the liver macrophages.

4. Conclusions

Taken together, the imaging and distribution studies reported herein of the tested HA NP formulations containing ICG, siRNA or cisplatin, were found consistent with the efficacy data reported earlier. In the previous efficacy studies, the HA-ODA NPs were chosen for cisplatin delivery, based on their slightly favorable tumor growth suppression at early time points compared to HA-ODA/HA-PEG NP formulation. But the present pharmacokinetic study suggests that the amount of cisplatin accumulated in tumor is very similar with both NP treatment. Although the trend showed that there was a decrease in cisplatin levels in tumors from 6 to 24 h when HA-ODA/HA-PEG NPs were used compared to the increase in levels observed with HA-ODA NPs, the numbers were not statistically different. Apart from this, the present study suggests that the HA-ODA NPs may have a favorable property for cisplatin delivery in terms of toxicity/safety with HA-ODA NP displaying significantly lower cisplatin levels in the liver at 24 h when compared to HA-ODA/HA-PEG NP formulation. Moreover, as demonstrated by whole body NIR ICG imaging and siRNA quantitation, the HA-PEI/HA-PEG NP designed specifically for siRNA delivery was able to target tumors expressing CD44 receptors at saturation levels with high residence time. Altogether, this study suggests that out of the systems analyzed, HA-ODA NP formulation may have favorable properties for safe and efficient targeted delivery of cisplatin to tumors while the HA-PEI/HA-PEG NP was efficient in delivering siRNAs to resistant lung cancer overexpressing CD44 receptors. The current findings demonstrate that utility of customizable HA based NPs for designing delivery systems for diverse payloads such as

cisplatin as well as siRNAs that have shown promising efficacy in combination treatments against resistant cancers.

Acknowledgments

This study was supported by a grant from the National Cancer Institute Alliance for Nanotechnology in Cancer's Platform Partnership (CNPP) grant U01-CA151452. The authors wish to thank Prof. William Zamboni and his research group at the University of North Carolina (UNC) at Chapel Hill, NC for quantitating the platinum content in the biological samples by ICP-MS. The authors also wish to thank Dr. Michael Beverly from Novartis Institutes for Biomedical Research, Cambridge, MA, for assisting in the design of the siRNA quantitation method.

References

1. Lage H. An overview of cancer multidrug resistance: a still unsolved problem. Cellular and molecular life sciences: CMLS. 2008; 65:3145–3167. [PubMed: 18581055]
2. Susa M, Iyer AK, Ryu K, Hornicek FJ, Mankin H, Amiji MM, Duan Z. Doxorubicin loaded Polymeric Nanoparticulate Delivery System to overcome drug resistance in osteosarcoma. BMC cancer. 2009; 9:399. [PubMed: 19917123]
3. Susa M, Iyer AK, Ryu K, Choy E, Hornicek FJ, Mankin H, Milane L, Amiji MM, Duan Z. Inhibition of ABCB1 (MDR1) expression by an siRNA nanoparticulate delivery system to overcome drug resistance in osteosarcoma. PloS one. 2010; 5:e10764. [PubMed: 20520719]
4. Yadav S, van Vlerken LE, Little SR, Amiji MM. Evaluations of combination MDR-1 gene silencing and paclitaxel administration in biodegradable polymeric nanoparticle formulations to overcome multidrug resistance in cancer cells. Cancer chemotherapy and pharmacology. 2009; 63:711–722. [PubMed: 18618115]
5. Ganesh S, Iyer AK, Weiler J, Morrissey DV, Amiji MM. Combination of siRNA-directed Gene Silencing With Cisplatin Reverses Drug Resistance in Human Non-small Cell Lung Cancer. Molecular therapy Nucleic acids. 2013; 2:e110. [PubMed: 23900224]
6. Ganesh S, Iyer AK, Morrissey DV, Amiji MM. Hyaluronic acid based self-assembling nanosystems for CD44 target mediated siRNA delivery to solid tumors. Biomaterials. 2013; 34:3489–3502. [PubMed: 23410679]
7. Saxena V, Sadoqi M, Shao J. Enhanced photo-stability, thermal-stability and aqueous-stability of indocyanine green in polymeric nanoparticulate systems. Journal of photochemistry and photobiology B, Biology. 2004; 74:29–38.
8. Saxena V, Sadoqi M, Shao J. Indocyanine green-loaded biodegradable nanoparticles: preparation, physicochemical characterization and in vitro release. International journal of pharmaceutics. 2004; 278:293–301. [PubMed: 15196634]
9. Sandanaraj BS, Gremlich HU, Kneuer R, Dawson J, Wacha S. Fluorescent nanoprobes as a biomarker for increased vascular permeability: implications in diagnosis and treatment of cancer and inflammation. Bioconjugate chemistry. 2010; 21:93–101. [PubMed: 19958018]
10. Hawrysz DJ, Sevick-Muraca EM. Developments toward diagnostic breast cancer imaging using near-infrared optical measurements and fluorescent contrast agents. Neoplasia. 2000; 2:388–417. [PubMed: 11191107]
11. Kitai T, Inomoto T, Miwa M, Shikayama T. Fluorescence navigation with indocyanine green for detecting sentinel lymph nodes in breast cancer. Breast Cancer. 2005; 12:211–215. [PubMed: 16110291]
12. Kim DE, Schellingerhout D, Jaffer FA, Weissleder R, Tung CH. Near-infrared fluorescent imaging of cerebral thrombi and blood-brain barrier disruption in a mouse model of cerebral venous sinus thrombosis. Journal of cerebral blood flow and metabolism: official journal of the International Society of Cerebral Blood Flow and Metabolism. 2005; 25:226–233. [PubMed: 15678125]
13. Li J, Makrigiorgos GM. Anti-primer quenching-based real-time PCR for simplex or multiplex DNA quantification and single-nucleotide polymorphism genotyping. Nature protocols. 2007; 2:50–58.

14. Stratford S, Stec S, Jadhav V, Seitzer J, Abrams M, Beverly M. Examination of real-time polymerase chain reaction methods for the detection and quantification of modified siRNA. Analytical biochemistry. 2008; 379:96–104. [PubMed: 18501185]
15. Kolishetti N, Dhar S, Valencia PM, Lin LQ, Karnik R, Lippard SJ, Langer R, Farokhzad OC. Engineering of self-assembled nanoparticle platform for precisely controlled combination drug therapy. Proceedings of the National Academy of Sciences of the United States of America. 2010; 107:17939–17944. [PubMed: 20921363]
16. Bosch ME, Sanchez AJ, Rojas FS, Ojeda CB. Analytical methodologies for the determination of cisplatin. Journal of pharmaceutical and biomedical analysis. 2008; 47:451–459. [PubMed: 18343619]
17. Paraskar AS, Soni S, Chin KT, Chaudhuri P, Muto KW, Berkowitz J, Handlogten MW, Alves NJ, Bilgicer B, Dinulescu DM, Mashelkar RA, Sengupta S. Harnessing structure-activity relationship to engineer a cisplatin nanoparticle for enhanced antitumor efficacy. Proceedings of the National Academy of Sciences of the United States of America. 2010; 107:12435–12440. [PubMed: 20616005]
18. Bahmani B, Lytle CY, Walker AM, Gupta S, Vullev VI, Anvari B. Effects of nanoencapsulation and PEGylation on biodistribution of indocyanine green in healthy mice: quantitative fluorescence imaging and analysis of organs. International journal of nanomedicine. 2013; 8:1609–1620. [PubMed: 23637530]
19. Zheng C, Zheng M, Gong P, Jia D, Zhang P, Shi B, Sheng Z, Ma Y, Cai L. Indocyanine green-loaded biodegradable tumor targeting nanoprobes for in vitro and in vivo imaging. Biomaterials. 2012; 33:5603–5609. [PubMed: 22575835]
20. Desmettre T, Devoisselle JM, Mordon S. Fluorescence properties and metabolic features of indocyanine green (ICG) as related to angiography. Survey of ophthalmology. 2000; 45:15–27. [PubMed: 10946079]
21. Jiang G, Park K, Kim J, Kim KS, Hahn SK. Target specific intracellular delivery of siRNA/PEI-HA complex by receptor mediated endocytosis. Molecular pharmaceutics. 2009; 6:727–737. [PubMed: 19178144]
22. Jadin L, Bookbinder LH, Frost GI. A comprehensive model of hyaluronan turnover in the mouse. Matrix biology: journal of the International Society for Matrix Biology. 2012; 31:81–89. [PubMed: 22142621]
23. Kennel SJ, Lankford TK, Foote LJ, Shinpock SG, Stringer C. CD44 expression on murine tissues. Journal of cell science. 1993; 104(Pt 2):373–382. [PubMed: 8505366]
24. Park K. To PEGylate or not to PEGylate, that is not the question. Journal of controlled release: official journal of the Controlled Release Society. 2010; 142:147–148. [PubMed: 20096317]
25. Perry JL, Reuter KG, Kai MP, Herlihy KP, Jones SW, Luft JC, Napier M, Bear JE, DeSimone JM. PEGylated PRINT nanoparticles: the impact of PEG density on protein binding, macrophage association, biodistribution, and pharmacokinetics. Nano letters. 2012; 12:5304–5310. [PubMed: 22920324]
26. Zamboni WC. Liposomal, nanoparticle, and conjugated formulations of anticancer agents. Clinical cancer research: an official journal of the American Association for Cancer Research. 2005; 11:8230–8234. [PubMed: 16322279]
27. Schiffelers RM, Ansari A, Xu J, Zhou Q, Tang Q, Storm G, Molema G, Lu PY, Scaria PV, Woodle MC. Cancer siRNA therapy by tumor selective delivery with ligand-targeted sterically stabilized nanoparticle. Nucleic acids research. 2004; 32:e149. [PubMed: 15520458]
28. Comenge J, Sotelo C, Romero F, Gallego O, Barnadas A, Parada TG, Dominguez F, Puntes VF. Detoxifying antitumoral drugs via nanoconjugation: the case of gold nanoparticles and cisplatin. PloS one. 2012; 7:e47562. [PubMed: 23082177]
29. Li SD, Howell SB. CD44-targeted microparticles for delivery of cisplatin to peritoneal metastases. Molecular pharmaceutics. 2010; 7:280–290. [PubMed: 19994852]
30. He C, Hu Y, Yin L, Tang C, Yin C. Effects of particle size and surface charge on cellular uptake and biodistribution of polymeric nanoparticles. Biomaterials. 2010; 31:3657–3666. [PubMed: 20138662]

Figure 1A.

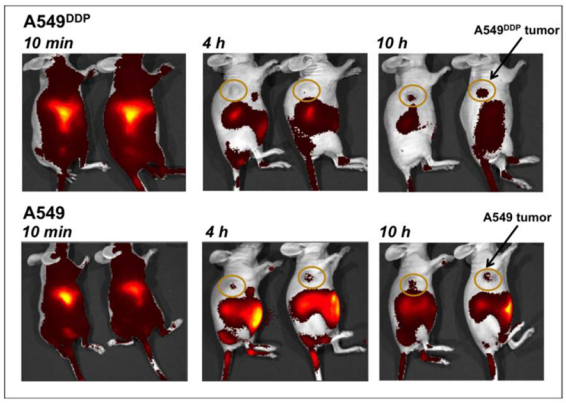

Figure 1B.

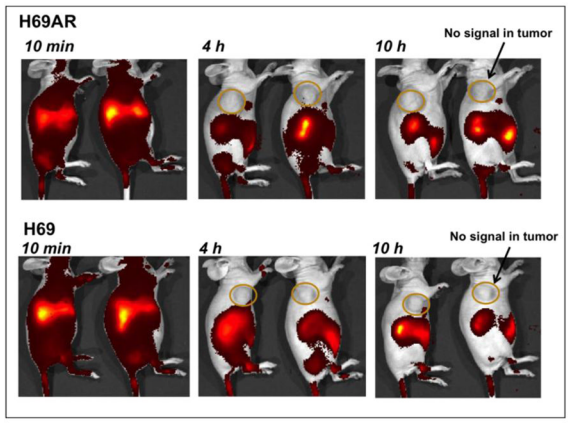

Figure 1C.

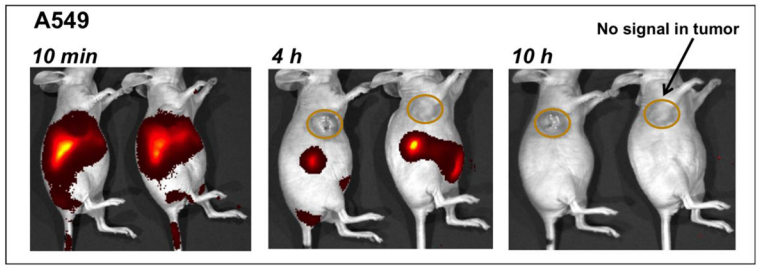

Figure 1. Whole body optical imaging

The distribution of indocyanine green-encapsulated hyaluronic acid-poly(ethylene imine)/ hyaluronic acid-poly(ethylene glycol) self-assembled nanoparticles (ICG/HA-PEI/PEG NP) in A549/ A549^{DDP} non-small cell lung cancer (A) and H69/H69AR small cell lung cancer (B) bearing mice is shown. Mice bearing A549 andA549^{DDP} and H69/H69AR tumors were injected with ICG/HA-PEI/PEG NPs and imaged at different time points using IVIS live imaging system. In order to see the half-life of ICG alone in circulation, the free dye ICG, was injected in A549 tumor bearing mice and imaged at different time points as shown (C).

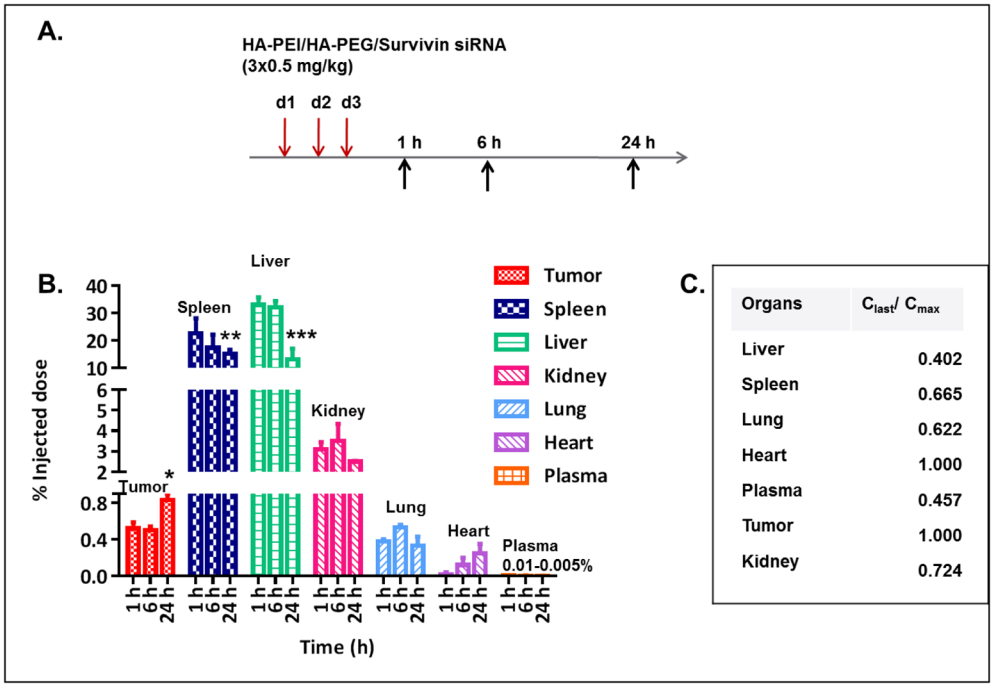

Figure 2. Study design and tissue distribution of siRNA-encapsulated hyaluronic acid nanoparticles in A549^{DDP} tumor bearing mice

The study was designed to mirror the same doses that were used in the efficacy studies. Tumor bearing mice were injected three times with survivin-silencing small interfering RNA-encapsulated in hyaluronic acid-poly(ethylene imine)/hyaluronic acid-poly(ethylene glycol) self-assembled nanoparticles (siRNA/HA-PEI/HA-PEG NP) at the siRNA dose of 0.5mg/kg. The organs and tissues were collected at 1 h, 6 h and 24 h after the last dose (A). A sensitive PCR method was utilized to quantitate the siRNA in tissue samples. The data is presented as % input dose/organ (B). The rate of siRNA elimination from the various organs and tissues were compared by calculating the C_{last}/ C_{max} values as shown (C). Indicated values were mean ± SE (n=3)$^{***}p<0.05$ compared to the liver siRNA amount at 1 h and 6 h time points, $^{**}p=0.08$ compared to the spleen siRNA amount at 1 h and 6 h time points, $^{*}p<0.05$ compared to the tumor siRNA amount at 1 h and 6 h time points.

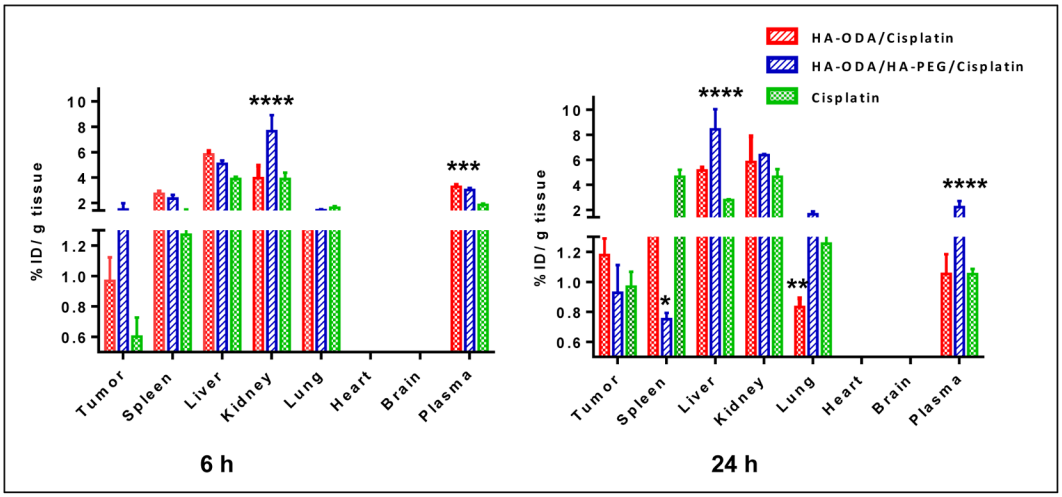

Figure 3. Tissue distribution of cisplatin and cisplatin-encapsulated hyaluronic acid nanoparticles in A549^{DDP} tumor bearing mice

Tumor bearing mice were injected with cisplatin or cisplatin encapsulated in hyaluronic acid-octyldiamine (HA-ODA) or HA-ODA/hyaluronic acid-poly(ethylene glycol) (HA-PEG) nanoparticles at 1 mg/kg (cisplatin dose). The tissues were collected at 6 h (A) and 24 h (B) post treatment. Inductively coupled-mass spectrometry (ICP-MS) was utilized to accurately quantitate the cisplatin concentrations in tissues. The data is presented as % input dose/g of tissue (% ID/g). Indicated values were mean ± SE (n=3).

**** $p<0.05$ compared to HA-ODA/cispaltin and cisplatin treated mice, *** $p<0.05$ compared to cispaltin treated mice, ** $p<0.01$ compared to HA-ODA/HA-PEG/cisplatin and cisplatin treated mice, * $p<0.01$ compared HA-ODA/cisplatin and cisplatin treated mice

Table 1
ICG-loaded hyaluronic acid nanoparticle characterization and study design

Indocyanine green-encapsulated hyaluronic acid-poly(ethylene imine)/hyaluronic acid-poly(ethylene glycol) self-assembled nanoparticles (ICG/HA-PEI/PEG NP) were prepared and the particle size, charge and % ICG loading was determined (A). ICG/HA-PEI/HA-PEG NPs were used in the distribution study to mirror the same system that was used in the efficacy studies for siRNA delivery. The study was designed to give a single dose equivalent of 0.5 mg/kg siRNA dose and to monitor the NIR signal at different times (B).

A.

	Size (nm)	Charge (mV)	% ICG loading (w/w)
HA-PEI/HA-PEG/ICG	200 ± 5.5	-14.6 ± 2.1	25

B.

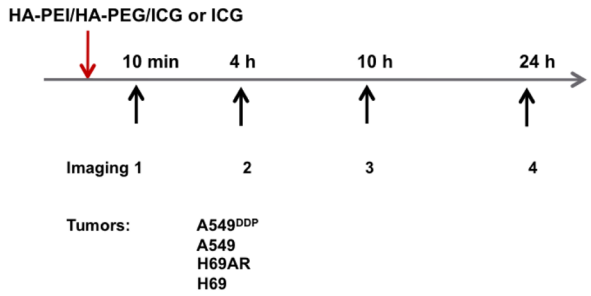

Table 2

Cisplatin-loaded hyaluronic acid nanoparticle characterization and study plan to determine the distribution

Cisplatin was encapsulated in hyaluronic acid-octyldiamine (HA-ODA) NP or in in HA-ODA/hyaluronic acid-poly(ethylene glycol) (HA-PEG) nanoparticles. The particle size, charge and % cisplatin loading was determined (A). The study design describes the doses and the timing at which the samples were collected for platinum analysis using ICP-MS (B).

A.

	Size (nm)	Charge (mV)	% Cisplatin loading (w/w)
HA-ODA/Cisplatin	~400 ± 7.2	-26.4 ± 4.5	~18
HA-ODA/HA-PEG/Cisplatin	~425 ± 5.5	-25.0 ± 3.5	~20

B.

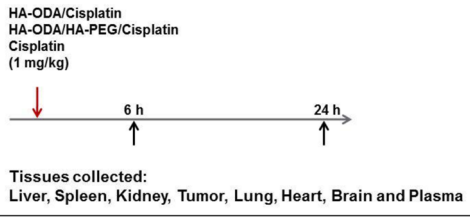

Table 3

Comparisons of C_{24h}/C_{6h} ratios to compare cisplatin residence in tissues upon administration in hyaluronic acid nanoparticles

Cisplatin was encapsulated in hyaluronic acid-octyldiamine (HA-ODA) NP or in HA-ODA/hyaluronic acid-poly(ethylene glycol) (HA-PEG) nanoparticles. The ratios of tissue cisplatin concentrations at 24 hours post-administration to 6 hours post-administration upon delivery in HA nanoparticles were compared with cisplatin administered in solution in $A549^{DDP}$ tumor bearing mice. Indicated values were mean ± SE (n=3).

C24h/ C6h	HA-ODA	HA-ODA/HA-PEG	Cisplatin
Plasma	0.323 ± 0.06	0.736 ± 0.2	0.568 ± 0.05
Tumor	1.216 ± 0.14	0.630 ± 0.22	1.609 ± 0.24
Liver	0.884 ± 0.05	1.659 ± 0.49	0.715 ± 0.03
Spleen	0.496 ± 0.04	0.321 ± 0.06	3.650 ± 1.2
Kidney	1.467 ± 0.07	0.832 ± 0.17	1.197 ± 0.48
Lung	0.629 ± 0.16	1.159 ± 0.25	0.775 ± 0.14
Brain	-	-	-
Heart	-	-	0.717 ± 0.21